Experimental Studies of Spatial Signature Variation at 900 MHz for Smart Antenna Systems

Shiann-Shiun Jeng, Guanghan Xu, *Member, IEEE*, Hsin-Piao Lin, and Wolfhard J. Vogel, *Fellow, IEEE*

***Abstract*—A spatial signature is the response vector of a base-station antenna array to a mobile unit at a certain location. Mobile subscribers at different locations exhibit different spatial signatures. The exploitation of spatial diversity (or the difference of spatial signatures) is the basic idea behind the so-called space-division multiple-access (SDMA) scheme, which can be used to significantly increase the channel capacity and quality of a wireless communication system. Although SDMA schemes have been studied by a number of researchers [1]–[6], most of these studies are based on theoretical analyses and computer simulations with ideal assumptions. Not much experimental study [7], [8] has been reported on spatial signature variation due to nonideal perturbations in a real wireless communication environment. The purpose of this paper is to present, for the first time, extensive experimental results of spatial signature variation using a smart antenna testbed. The results to be presented include the spatial signature variation with time, frequency, small displacement, multipath angle spread and beamforming performance. The experimental results show the rich spatial diversity and potential benefits of using an antenna array for wireless communication applications.**

***Index Terms*—Adaptive arrays, mobile communication.**

I. Background

DEMAND for wireless communications has grown exponentially during the last five years. With such rapid growth, the most important problem for wireless communications is how to increase channel capacity. Besides the capacity problem, the drastic increase of radio traffic also worsens existing difficulties, such as multipath, channel reuse among neighboring cells, near–far receiving problems, handoff from one cell base station to another, limited battery life for pocket handsets, etc.

Different schemes have been proposed to increase the number of users in a fixed spectrum slot. Frequency division multiple access (FDMA) assigns each user to transmit on a separate frequency band in the same time slot. Time division multiple access (TDMA) assigns each user to transmit during a different time slot while sharing the same frequency band. Code division multiple access (CDMA) assigns a unique code to each user to encode the transmitted signal and allows multiple users to share the same frequency band and the same time slot. Although these approaches do significantly increase the channel capacity, each scheme basically is attempting, in its own way, a more efficient use of the same resource. Since radio-frequency (RF) bandwidth is a limited resource, these techniques have approached their fundamental limitations. Other proposals such as microcells have also been suggested. Though the channel capacity can be increased to some extent by subdivision, it is very costly, involves more cell sites, and too frequent handoffs.

Since different mobile users transmit from and receive at different spatial locations, besides frequency, time, and code diversities, there is very rich spatial diversity that can be exploited to significantly increase the system capacity as well as improve the system performance. However, this spatial diversity is not exhibited a traditional single-antenna system, but rather requires the use of spatially separated multiple antennas or an antenna array. Therefore, any SDMA system must have an antenna array at a base station to exploit the spatial diversity among different users. Many existing and new array-signal processing techniques are being proposed for the SDMA scheme, but most of the performance evaluation to date relies on computer simulations or theoretical analyses based on ideal assumptions. No spatial signature variations due to the channel propagation effect have yet been taken into account, although the channel propagation effect is critically important to the design engineer of an SDMA system. For example, the variation of the spatial signature due to motion may help her determine the appropriate update rate of the spatial signature. The purpose of this paper is to describe various propagation experiments carried out in typical scenarios, to derive the spatial signature and direction of arrival (DOA) variations and to demonstrate the rich spatial diversity and potential benefits of using an antenna array for wireless communications.

II. Description of Spatial Signatures

A. Brief Description of an SDMA System

Fig. 1 shows the basic implementation architecture of a smart antenna system. The signal received by the antenna array is processed with advanced signal processing algorithms and the signal of interest is extracted from the received waves by exploiting the spatial diversity between the signal of interest and other signals, such as co-channel

Manuscript received June 3, 1996; revised February 25, 1997. This work was supported in part by the NSF CAREER Award under Grant MIP-9502695, the Office of Naval Research under Grant N00014-95-1-0638, the Joint Services Electronics Program under Contract F49620-95-C-0045, Motorola, Inc., Southwestern Bell Technology Resources, Inc., and Texas Instruments.

S.-S. Jeng and G. Xu are with the Department of Electrical and Computer Engineering, The University of Texas at Austin, Austin, TX 78712 USA.

H.-P. Lin and W. J. Vogel are with the Electrical Engineering Research Lab., J. J. Pickle Research Campus, University of Texas at Austin, Austin, TX 78758 USA.

Publisher Item Identifier S 0018-926X(98)05771-8.

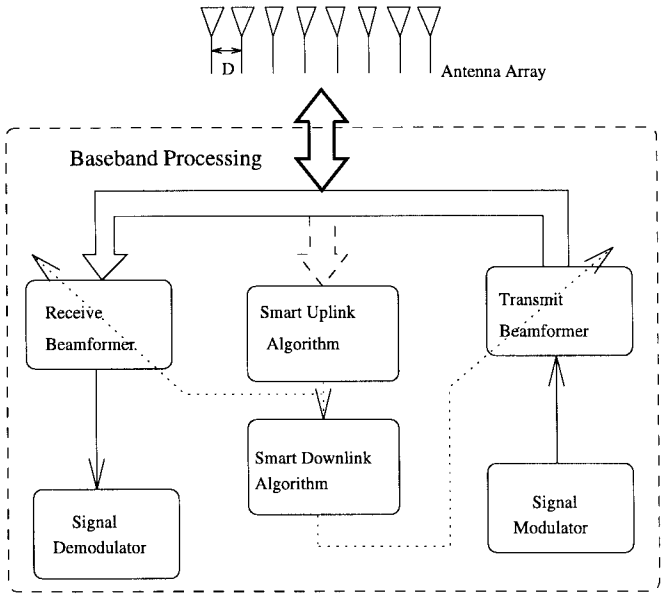

Fig. 1. Implementation diagram of an SDMA base station.

interference or background noise. Spatial diversity is actually the difference of the so-called *spatial signatures* of mobile terminals. The definition of spatial signatures is given below. Spatial diversity can also be exploited to generate transmit beamforming patterns such that each signal is delivered to its desired location with minimum interference to other users. Of course, the uplink and downlink algorithms vary with the multiplexing schemes e.g., FDMA, TDMA, and CDMA and duplexing schemes, e.g., time-division duplex (TDD) and frequency-division duplex (FDD).

B. Definition of Spatial Signatures

At a base station, an M-element antenna array receives signals from several spatially separated users. The received waves typically contain both direct path and multipath signals, which are most likely from different directions of arrival. Let us assume that the array response vector to a transmitted signal $s_1(t)$ from a direction of arrival θ is $\mathbf{a}(\theta) = [1, a_1(\theta), \cdots, a_M(\theta)]^T$, where $a_i(\theta)$ is a complex number denoting the amplitude gain and phase shift of the signal at the $(i+1)$th antenna relative to the first antenna. For a uniform linear array in free-space with separation D (as shown in Fig. 2) $\mathbf{a}(\theta) = [1, e^{j2\pi f \sin\theta D/c}, \cdots, e^{j2\pi f \sin\theta (M-1)D/c}]^T$, where f, c, and T denote the carrier frequency, speed of light, and transpose operator, respectively. In a typical wireless scenario, the antenna array comprised of omnidirectional elements not only receives a signal $s_1(t)$ propagated along the direct path, but also many multipath echoes with different DOA's. Therefore, the total signal vector received by the antenna array can be written as

$$\mathbf{x}(t) = \underbrace{\mathbf{a}(\theta_1)s_1(t)}_{\text{direct path}} + \underbrace{\sum_{l=2}^{N_m} \alpha_l \mathbf{a}(\theta_l)s_1(t)}_{\text{multipath}} = \mathbf{a}_1 s_1(t) \qquad (1)$$

where $N_m - 1$ is the total number of multipath signals, α_l is the phase and amplitude difference between the lth multipath and the direct path, and $\mathbf{a}_1 = \sum_{l=1}^{N_m} \mathbf{a}(\theta_l)$, which is referred to as the *spatial signature* or SS, is associated with source one.

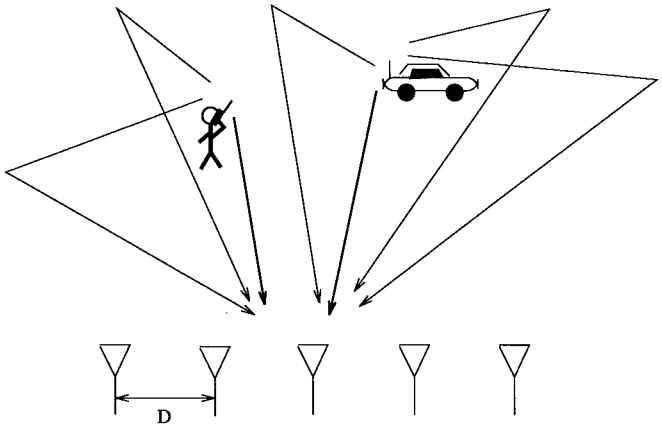

Fig. 2. A uniform linear antenna array and two co-channel sources.

If there are d sources sharing the same frequency band and time slot, then the signal received by the antenna array is

$$\mathbf{x}(t) = \sum_{k=1}^{d} \mathbf{a}_k s_k(t) + \mathbf{n}(t), \qquad (2)$$

where $\mathbf{n}(\cdot)$ is background noise and other uncorrelated interference.

If there are long-delay multipath components present,[1] both spatial and time diversity can be exploited using SDMA and rake receivers, respectively. For narrowband signals such as TDMA or FDMA signals, however, most multipath components do not have significant long-delay multipath in real scenarios. Consequently, the difference in the spatial signatures among different mobile users is the only diversity that can be exploited. The effectiveness of SDMA systems rely heavily on the characteristics of spatial signatures. The main purpose of this paper is to experimentally characterize the spatial signatures in some typical wireless communication scenarios.

C. Calculation of Spatial Signatures and Their Variations

If there is only one source present, as assumed in (1), the data vector received by the antenna array can be written as

$$\mathbf{x}(t) = \mathbf{a}_1 s_1(t) + \mathbf{n}(t) \qquad (3)$$

where $\mathbf{a}_1$ is the spatial signature and $\mathbf{n}(\cdot)$ is background noise. Suppose that $\mathbf{n}(\cdot)$ is spatially white noise, i.e., the correlation of the noise between two antenna elements is zero. Then the spatial signature can be easily obtained via a singular value decomposition (SVD) of the data matrix $\mathbf{X} = [\mathbf{x}(1), \cdots, \mathbf{x}(N)]$ or an eigenvalue decomposition of the sample covariance matrix, i.e., $\mathbf{R}_x = \frac{1}{N}\mathbf{X}\mathbf{X}^*$, where $*$ denotes the complex conjugate and transpose operation.

Since the spatial signature is a vector instead of a scalar, it is more difficult to characterize its variation. Here, we quantify

[1] Long-delay multipath means multipath with time delay comparable to the signal symbol period or the inverse of the signal bandwidth.

its variation by measuring both relative amplitude and angle changes. The *relative angle change* of two spatial signatures $\mathbf{a}_i$ and $\mathbf{a}_j$ is defined as

$$\text{Relative Angle Change (\%)} = 100 \times \sqrt{1 - \left| \frac{\mathbf{a}_i^*}{||\mathbf{a}_i||} \cdot \frac{\mathbf{a}_j}{||\mathbf{a}_j||} \right|^2} \tag{4}$$

Also, *the relative amplitude change* of two spatial signatures $\mathbf{a}_i$ and $\mathbf{a}_j$ can be represented as

$$\text{Relative Amplitude Change (dB)} = 20 \log_{10} \frac{||\mathbf{a}_j||}{||\mathbf{a}_i||} \tag{5}$$

where $||\mathbf{b}||$ denotes the norm of vector $\mathbf{b}$.

The relative angle change defined in (4) helps determine the update rate of the weight vectors for downlink beamforming. For example, in a TDD system where the uplink and downlink share the same carrier, we can design and keep a weight vector of a smart antenna system based on the spatial signature received at the ith time slot such that $\mathbf{w} = \mathbf{a}_i^*$ for the downlink. At the jth time slot, the signal received by the mobile user will be $(\mathbf{a}_i^* \mathbf{a}_j) s(t)$, where $\mathbf{a}_i$ and $\mathbf{a}_j$ are normalized vectors. If the update rate is fast enough so that $|\mathbf{a}_i^* \mathbf{a}_j| \approx 1$ or the relative angle change $\approx 0\%$, the mobile user will receive the maximum signal power. However, if the update rate is slow so that $|\mathbf{a}_i^* \mathbf{a}_j| \approx 0$ or the relative angle change $\approx 100\%$, the mobile user will not receive any signal power, causing deep fading.

The relative amplitude change defined in (5) gives the relative signal power that can be received from an incident field with spatial signature $\mathbf{a}_j$ at the jth time slot relative to the signal power received with spatial signature $\mathbf{a}_i$ at the ith time slot. This definition is very similar to the standard definition of multipath fading seen by a single antenna.

D. Direction-of-Arrival Estimation

As explained in (1),

$$\mathbf{a}_1 = \underbrace{\mathbf{a}(\theta_1)}_{\text{direct path}} + \underbrace{\sum_{l=2}^{N_m} \alpha_l \mathbf{a}(\theta_l)}_{\text{multipath}} \tag{6}$$

the spatial signature $\mathbf{a}_1$ is a linear combination of the different array response vectors for the direct path and the multipath signals. It obviously depends on the DOA's of the direct path and multipath components. Therefore, the effect of multipath DOA's on spatial signatures was also studied experimentally. The high-resolution direction finding algorithm ESPRIT [9] was used to find direct path and multipath DOA's in our experiments. Since multipath signals are sources coherent with the direct path, the signal eigenvectors will fail to span the signal subspace and loss of rank in the signal subspace causes the ESPRIT algorithm to fail. In order to restore the dimensionality of the signal subspace, the forward and backward spatial smoothing scheme [10], [11] was used to decorrelate the coherence among multipath signals. The penalty for using the extended approach is that it can only estimate up to $(2/3)M$ DOA's of multipath and direct path components, where M is the number of antennas.

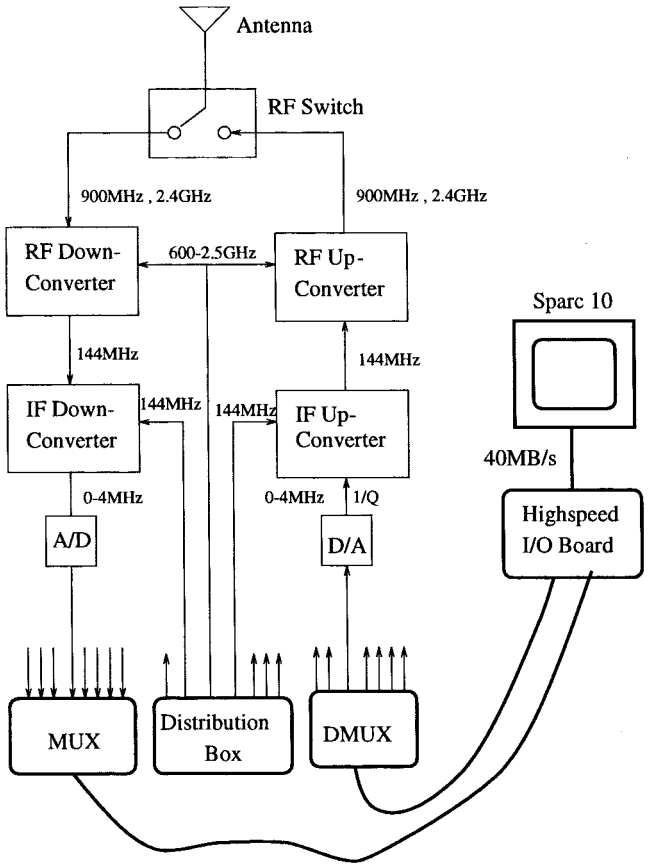

Fig. 3. A diagram of one channel of the smart antenna system.

III. Experimental Setup

A. The Smart Antenna Testbed

A variety of experiments were carried out using the smart antenna testbed shown in Fig. 3. The testbed is comprised of the following subsystems: 1) one eight-element patch antenna array and four one-element dipole antennas. The eight-element patch antenna array, arranged in a linear fashion with separation of about one-half wavelength, is the base-station antennas. The dipole antennas are used by four mobile units; 2) 12 RF and intermediate frequency (IF) up/down converters and switches operating in the RF band at around 900 MHz and IF band at around 144 MHz; 3) two distribution boxes providing synthesized sources for RF and IF local oscillator signals; 4) 12 A/D's and 24 D/A's; 5) four digital multiplexing (MUX) and demultiplexing (DEMUX) boards. All MUX/DEMUX boards are connected to a Sparc 10 workstation; 6) two bi-directional high-speed input/output boards installed in the s-bus slots of a Sparc 10 workstation.

The system is very stable with time and temperature. The spatial signature variation due to equipment effects was determined to be less than 1% relative angle change and ± 0.06 dB relative amplitude change over the duration of a typical measurement. A system calibration was performed before and after each propagation experiment.

Fig. 4. Indoor experimental environment (view from the antenna array).

Fig. 5. Indoor experimental environment (view from the mobile terminal).

Fig. 6. Outdoor experimental environment (view from the antenna array).

B. Experimental Environment

We conducted a series of spatial signature variation measurements inside and outside of the Electrical Engineering Research Laboratory (EERL) at the J. J. Pickle Research Campus, University of Texas at Austin. Photographs of some of the measurement sites are shown in Figs. 4–7. The indoor environment is a rectangular shaped one-story building with several office rooms partitioned with lumber and concrete-block construction and a large laboratory also containing a shielded room with a metal door. The building is equipped with various microwave and electronic instruments, personal computers and peripherals, an assortment of cables, wooden and metal desks, file cabinets, a van for mobile communications measurements, and book shelves. The outdoor environment is a paved area surrounded by several buildings and metal chain-link fences.

Fig. 7. Outdoor experimental environment (view from the mobile terminal).

IV. Experimental Results

A. Stability of Spatial Signature Variation

As explained above, the spatial signature represents the response of an array antenna to an emitter at a certain location in a given environment. In wireless communications, different mobile users are usually located in different positions and, therefore, have different spatial signatures at the base-station antenna array. Exploiting these differences of the spatial signatures, we can selectively receive and transmit multiple co-channel signals without creating interference among the users. To achieve a certain required level of isolation between two not widely separated sources in a typical scenario, one needs to know the stability of the spatial signature. For this purpose, we placed a fixed emitter first indoors and then outdoors and measured the spatial signatures over 8 h, taking one snapshot every 5 min. The results are shown in Figs. 8 and 9, which illustrate that the relative amplitude change of the spatial signature was within ± 1.2 dB, and that the relative angle change of the spatial signature was less than 14%. Thus, the spatial signatures do not vary significantly over a long period of time as long as the mobile unit is stationary. It is also apparent that the spatial signatures measured outdoors vary more than those measured indoors. Some of the spikes in the outdoors case may have been caused by moving objects, such as vegetation in the wind or passing vehicles. The outdoor environment cannot be maintained as stationary as the indoor environment for such a long time. It should be noted that the outdoor experimental environment was a research campus, which may have less traffic density than other environments. Furthermore, the indoor environment was

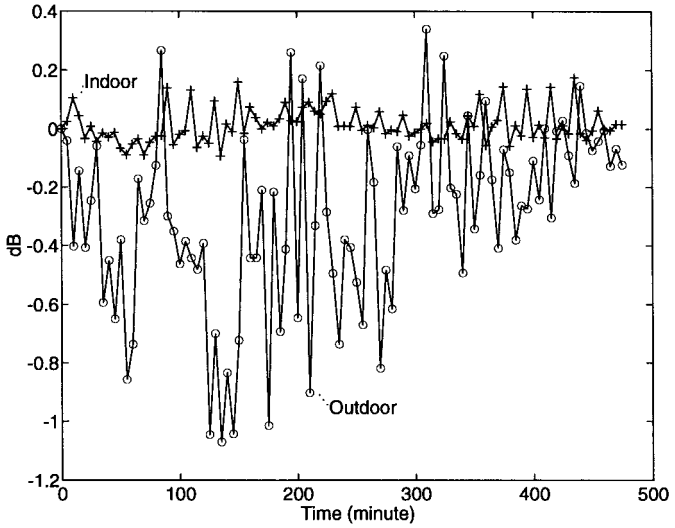

Fig. 8. Relative amplitude change of the spatial signature of a stationary emitter.

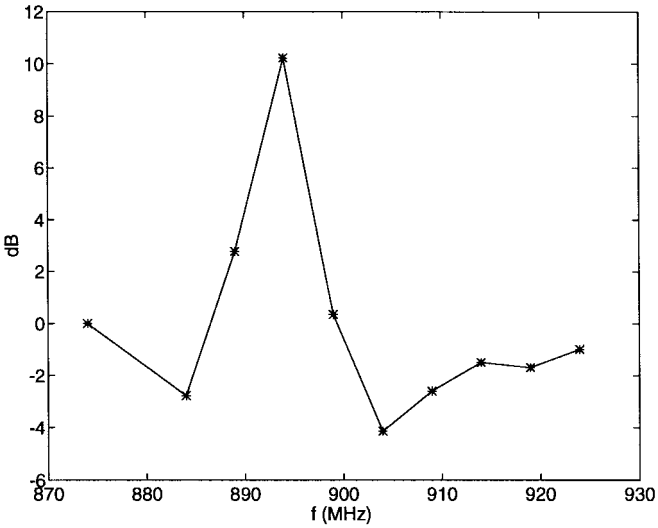

Fig. 10. Relative amplitude change of the spatial signature corresponding to different carrier frequencies.

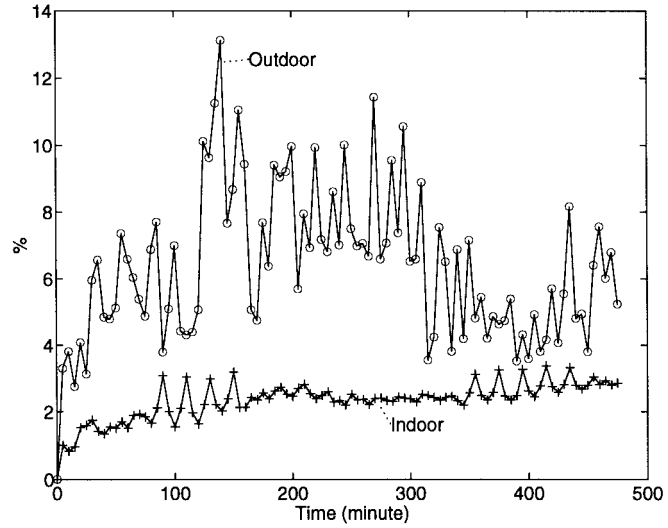

Fig. 9. Relative angle change of the spatial signature of a stationary emitter.

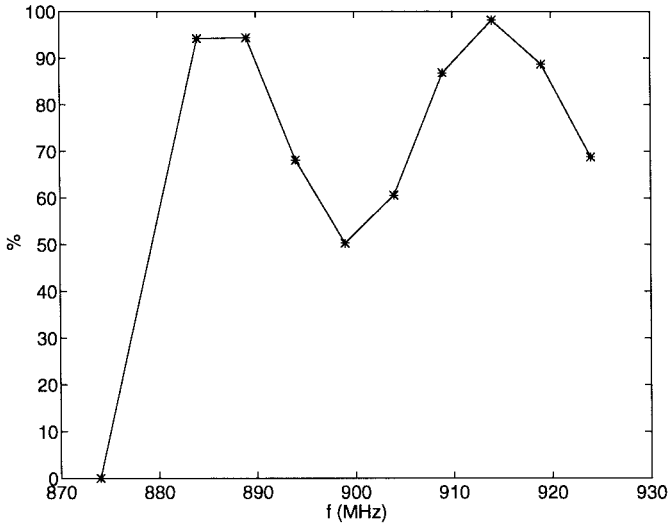

Fig. 11. Relative angle change of the spatial signature corresponding to different carrier frequencies.

a laboratory occupied by only five people at the time of the measurement. Other indoor environment may be busier. If the environment has greater traffic density, then we may expect more variation in the spatial signature.

B. Spatial Signature Variation with Frequency

In current cellular telephony near 800 MHz, downlink and uplink frequencies have about 45-MHz separation. It should, therefore, be interesting to determine the variation of the spatial signature across such a frequency difference. The result illuminates the feasibility (or lack thereof) to expand the capacity of the already existing infrastructure of reusing uplink spatial signatures for selective transmission in the downlink. In the experiment, we fixed the mobile's location and varied the carrier frequency from 874 to 924 MHz in 5-MHz steps. This measurement was made outdoors at a site with two dominant DOA's. Figs. 10 and 11 depict the variation of the spatial signature with carrier frequency. Obviously, the spatial signature variation is quite significant even for a small percentage change ($<5\%$) of the carrier frequency. This implies that the uplink spatial signature cannot be used directly for downlink beamforming in an FDD system.

C. Spatial Signature Variation Due to Small Displacement in Different Multipath Environments

It is well known that the fading rate of a mobile terminal is determined by its speed. One would also expect that the rate of spatial signature variation is proportional to terminal speed. This rate determines the beamforming update rate for an antenna array system. In our experiments, we chose three cases each for indoor and outdoor scenarios to study the rate of spatial signature variation with small displacement: 1) one strong DOA; 2) two strong DOA's; 3) many ($\geq$ 3) DOA's. In each case, we calculated the spatial signature variations by moving the transmitter along a line with a step size

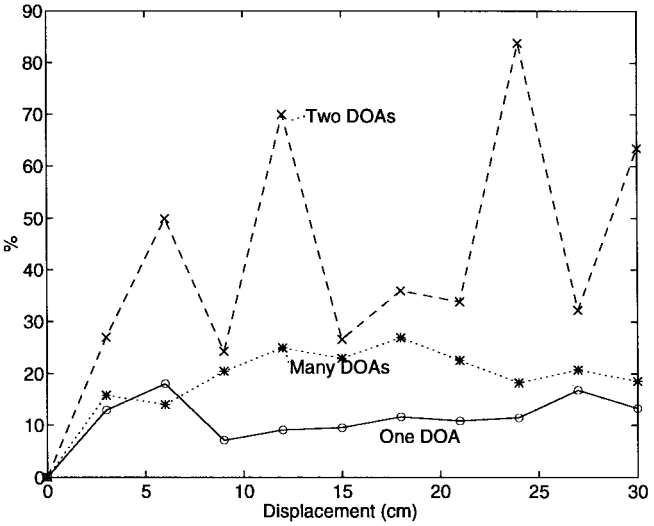

Fig. 12. Relative angle change of the spatial signature between adjacent positions in different indoor multipath scenarios with small displacement of the mobile terminal.

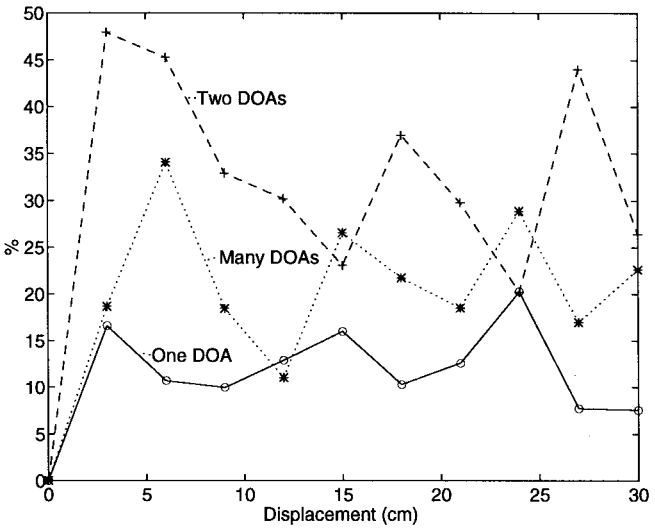

Fig. 14. Relative angle change of the spatial signature between adjacent positions in different outdoor multipath scenarios with small displacement of the mobile terminal.

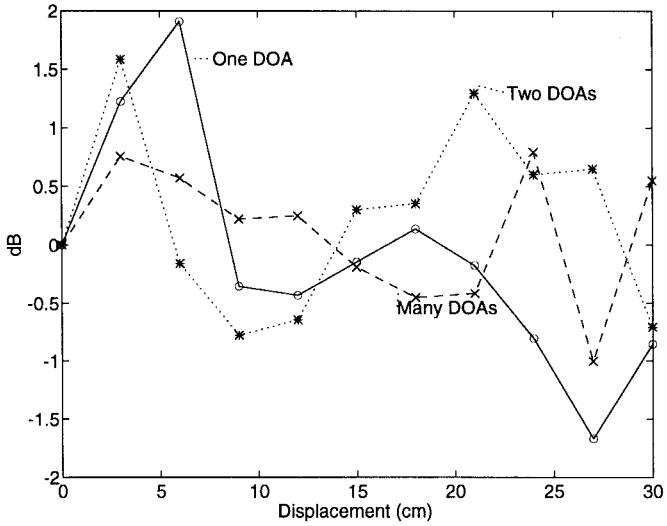

Fig. 13. Relative amplitude change of the spatial signature between adjacent positions in different indoor multipath scenarios with small displacement of the mobile terminal.

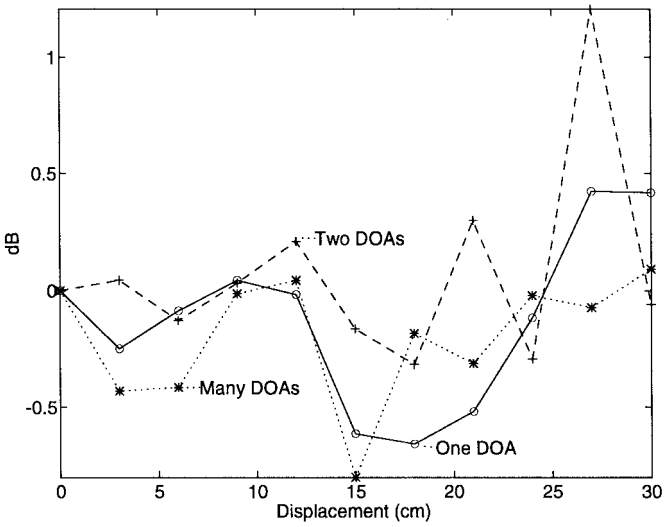

Fig. 15. Relative amplitude change of the spatial signature between adjacent positions in different outdoor multipath scenarios with small displacement of the mobile terminal.

of 3 cm (equivalent to about 0.1λ). The total displacement was 30 cm (equivalent to about 1λ). The relative angle and amplitude changes between two adjacent spatial signatures for the indoors and outdoors cases are shown in Figs. 12 and 13 and in Figs. 14 and 15, respectively. The mean and standard deviations of the relative angle and amplitude change for those three cases were also calculated and are listed in Table I. It should be noted that the results exhibited in Figs. 12–15 and Table I are typical cases, representing the range of spatial signature variations of all 23 sets of measurements taken.

From Figs. 12 and 14, we can see that the relative angle change in case 1), i.e., with one strong DOA, is much smaller than that in cases 2) and 3). This can be explained as follows: the spatial signature in case 1) is virtually a scalar multiple of $\mathbf{a}(\theta_1)$, while those in cases 2) and 3) are a linear combination of $\{\mathbf{a}(\theta_l)\}_{l=1}^{N_m}$, i.e., as given by (6). Although small displacement does not cause too much change of the amplitude of $\mathbf{a}(\theta_l)$, it does change the path

TABLE I
MEAN AND STANDARD DEVIATION OF THE RELATIVE ANGLE AND AMPLITUDE CHANGES IN DIFFERENT MULTIPATH SCENARIOS

		Relative Angle Change		Relative Amplitude Change	
		Mean	Std	Mean	Std
Indoor	One DOA	12.04 %	3.36 %	-0.12 dB	1.03 dB
	Two DOAs	44.69 %	20.98 %	0.11 dB	0.60 dB
	Many ($\geq$ 3) DOAs	20.49 %	4.01 %	0.25 dB	0.82 dB
Outdoor	One DOA	12.47 %	4.11 %	-0.14 dB	0.39 dB
	Two DOAs	33.68 %	9.60 %	0.08 dB	0.44 dB
	Many ($\geq$ 3) DOAs	21.77 %	6.62 %	-0.21 dB	0.28 dB

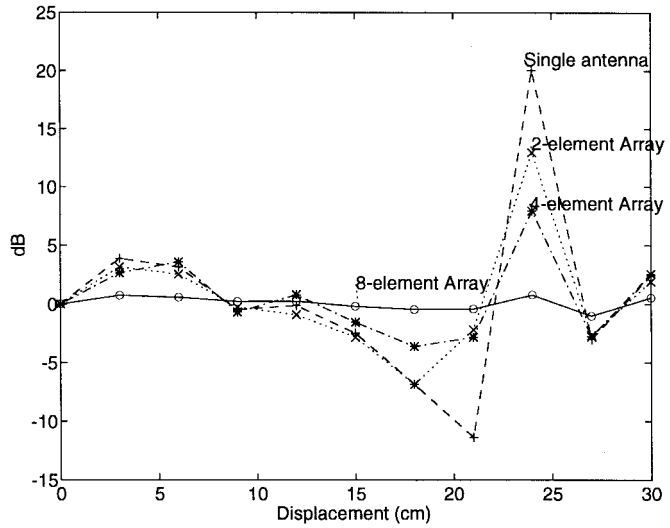

Fig. 16. Relative amplitude change of the received signal with a single antenna and an antenna array with two, four, or eight elements.

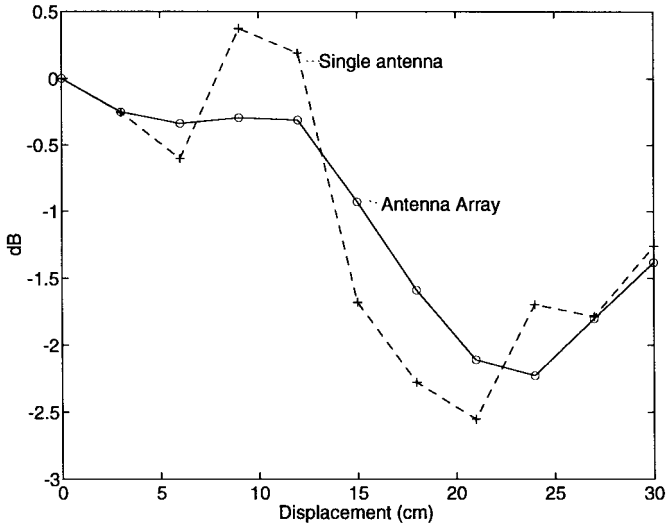

Fig. 17. Relative amplitude change of the received signal with a single antenna and an antenna array when there is only one dominant DOA and insignificant multipath.

length of each multipath component and, therefore, changes the phase α_l. Consequently, the spatial signature may also change significantly with small displacement of the mobile terminal. It is interesting to note that the spatial signature varies more significantly in case 2) than in case 3). One explanation is that the cancellation effect is stronger with two DOA's since the spatial signature may change from $\mathbf{a}(\theta_1) + \alpha_2\mathbf{a}(\theta_2)$ to $\mathbf{a}(\theta_1) - \alpha_2\mathbf{a}(\theta_2)$.

Figs. 13 and 15 confirm that the amplitude changes in all three cases are small—less than 4 dB. The mean and standard deviations of the relative amplitude changes are all less than 1.03 dB. These results demonstrate that a smart antenna system with an update rate faster than the rate of change of the propagation channel can, in most cases, mitigate multipath fading by exploiting spatial diversity. (The one exception is the case when there are many multipath components with similar DOA's, which will be discussed in the next section.) Fig. 16 further illustrates this point with a typical sample taken from the entire set of 23 measurements, comparing worst-case amplitude variations for a single antenna to those for an antenna array with two, four, and eight elements.

D. Multipath Angle Spread

The angle spread of multipath is generally defined as the maximum difference of DOA's among significant multipath components. The angle spread of multipath is critical to the multipath fading characteristics of an antenna array as well as the feasibility of using direction finding techniques for selective uplinks and downlinks. If the angle spread is small, i.e., $\theta_1 \approx \theta_2 \approx \cdots \approx \theta_{N_m}$, then by (1)

$$\mathbf{a}_1 = \mathbf{a}(\theta_1) + \sum_{l=2}^{N_m} \alpha_l \mathbf{a}(\theta_l) \approx \mathbf{a}(\theta_1)\left(1 + \sum_{l=2}^{N_m} \alpha_l\right). \quad (7)$$

In this case, the spatial signature is basically a scalar multiple of the array manifold $\mathbf{a}(\theta_1)$. This situation may be illustrated with the following two hypothetical scenarios: 1) there is only one direct path without any other significant multipath and 2) there are many multipath components with similar DOA's (localized scatterers). The fading characteristics of these two scenarios are completely different. In the first case, there is virtually no fading even with a single antenna, while in the latter case, fading can be quite severe even with an antenna array because the spatial diversity can not help much. To quantify these fading characteristics, we chose two canonical cases and measured relative amplitude changes. In the first case, the transmitter was placed in an open field at a distance from the base station of about 400 m. Since there was no scatterer close to the transmitter, only one dominant DOA was detected (the specular reflection has the same DOA). In the second case, the transmitter was set up in the parking lot close to a research building. The parking lot was nearly filled with cars, all acting as scatterers. Since the distance between the transmitter and the scatterers was small compared to the distance between the transmitter and the base station, we could view this as the case with many multipath components with similar DOA's. The relative amplitude changes are given in Figs. 17 and 18. Shown in Fig. 17 for case 1), the relative amplitude changes measured with either a single antenna or the antenna array were all less than 3 dB. There was no severe fading even with a single antenna; on the other hand, shown in Fig. 18 for case 2), the maximum relative amplitude change measured with the antenna array was up to 6 dB. Therefore, fading was very severe even with an antenna array.

In either case, DOA-based selective uplinks and downlinks may be quite effective, however, since direction diversity is the only diversity left to exploit. If the angle spread is large, the above conclusions are the opposite, i.e., direction finding based techniques are not that effective and the spatial diversity of multiple antennas can be exploited to combat multipath fading.

To find the DOA distribution in different environments, the following three cases were chosen for measurement of their multipath angle spread: 1) the base station and the mobile transmitter were put inside EERL's laboratory space, as shown

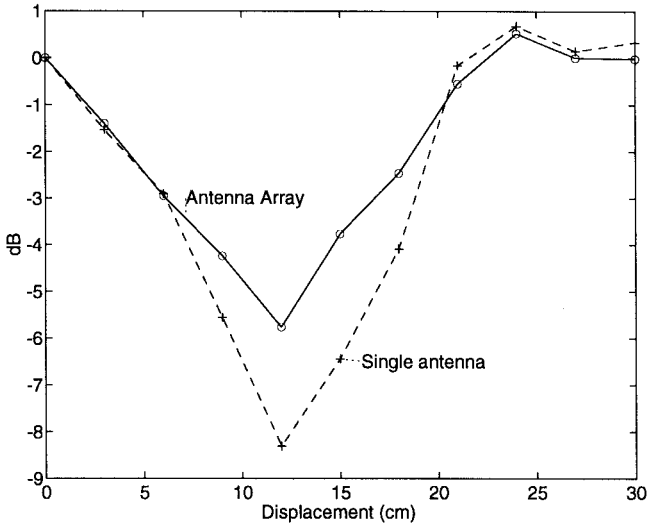

Fig. 18. Relative amplitude change of the received signal with a single antenna and an antenna array in the case of many multipath scatterers with similar DOA's.

TABLE II
MEAN AND STANDARD DEVIATION OF ANGLE SPREAD IN DIFFERENT SCENARIOS

		Intensity		
		$\geq -3dB$	$\geq -6dB$	$\geq -9dB$
Indoor	Mean	4.41°	10.01°	21.19°
	Std	8.67°	11.85°	22.97°
Outdoor	Mean	0.66°	4.01°	10.70°
(LOS)	Std	2.66°	7.36°	11.27°
Outdoor	Mean	15.47°	25.50°	39.28°
(Block)	Std	26.00°	26.04°	23.49°

TABLE III
RMS ANGLE SPREAD IN DIFFERENT SCENARIOS

	RMS Angle Spread
Indoor	10.03°
Outdoor (LOS)	7.02°
Outdoor (Blocked)	24.88°

in Fig. 4, for the indoor measurement; 2) The base station was placed outside EERL and the mobile transmitter was set up in an open field. There was nothing between the base station and the transmitter blocking the direct path of the outdoors line-of-sight (LOS) measurement; and 3) The base station was located outside EERL and the mobile transmitter was placed in a location where the LOS was blocked by a building. In each scenario, we randomly moved the mobile transmitter to several positions. At each position, the number and intensity of DOA's were detected by the ESPRIT algorithm and forward/backward spatial smoothing techniques. Limited by the number of array elements and the direction finding algorithm, we can reliably estimate at most, four major DOA's. In the experiments, we obtained and analyzed 102 sets of DOA data but only exhibit 40 typical cases measured at 16 positions for the indoors measurement, 16 positions for the outdoors LOS measurement, and eight positions for the outdoors blocked LOS measurement. At each position, we measured the DOA angle spread with signal level thresholds of -3 dB, -6 dB, and -9 dB. For this reason, we defined DOA spread as the maximum angle of arrival difference between the DOA of the direct path and any other DOA's whose intensity was higher than the specified threshold. The mean and standard deviation of angle spread results for all three cases and thresholds are summarized in Table II. From these results, we can see that the angle spread of outdoors LOS case was much smaller than that of the indoors and outdoors blocked cases. In the outdoors LOS environment, angle spread of multipath may be small since most significant multipath components are from local scatterers within 100–1000 wavelengths, which is small in comparison with the distance between the base station and the mobile terminal. This may not be true in an indoors environment. Since the path lengths of direct path and multipath components are not so different there, we expect to see more significant multipath components and wider angle spread. For the outdoors blocked environment, since there is no direct signal path, multipath components can be from scatterers in any direction. The angle spread of the significant multipath components is quite arbitrary in the blocked case. Therefore, the mean and standard deviation of angle spread are larger than those of the other two cases examined.

The root mean square (rms) angle spread, which takes into account the relative power of each multipath component, was calculated as

$$\text{RMS Angle Spread } (\sigma) = \frac{\sum_{i=1}^{P} \sqrt{\bar{\theta}_i^2 - (\bar{\theta}_i)^2}}{P} \qquad (8)$$

where

$$\bar{\theta}_i = \frac{\sum_{l=1}^{N_m} \|\alpha_{il}\|^2 \theta_{il}}{\sum_{l=1}^{N_m} \|\alpha_{il}\|^2}, \quad \bar{\theta}_i^2 = \frac{\sum_{l=1}^{N_m} \|\alpha_{il}\|^2 \theta_{il}^2}{\sum_{l=1}^{N_m} \|\alpha_{il}\|^2}$$

P is the total number of positions measured in each case, θ_{il} is the measured DOA and α_{il} represents the phase and amplitude difference between the lth multipath and the direct path at the ith position. The results are summarized in Table III. We can see that the rms angle-spread statistics shown in Table III are consistent with those shown in Table II.

The experimental results suggest that DOA-based techniques may not be so effective in indoors and outdoors blocked applications. We also have shown that multipath fading can be overcome by exploiting spatial diversity. However, if the angle spread is the result of some well defined specular components arriving at the smart antenna with a reasonably intelligent downlink beamforming strategy, some significant downlink improvement might still be achieved.

E. Feasibility of Downlink Beamforming

In TDD systems such as CT-2 and DECT, the carrier frequencies for uplinks and downlinks are the same. In this case, the uplink spatial signatures obtained from blind-type algorithms can be directly used for downlink beamforming. To verify this claim experimentally, we formed downlink weighting vectors based on the uplink spatial signatures of

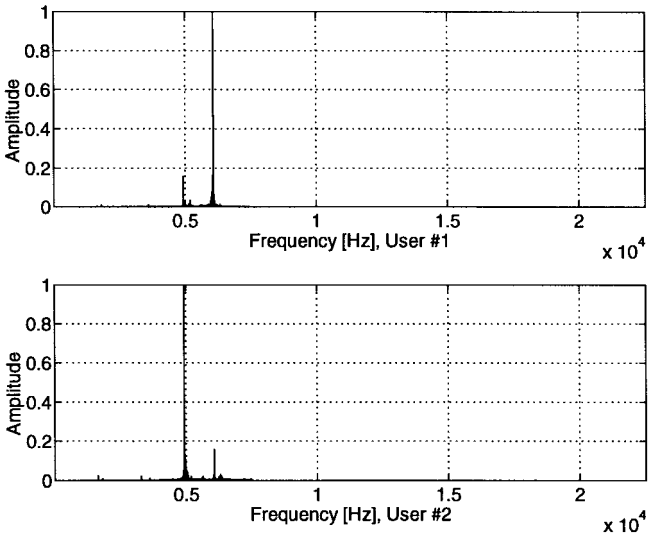

Fig. 19. Spatial-signature (SS)-based beamforming results for two sources with angular separation of about 20°.

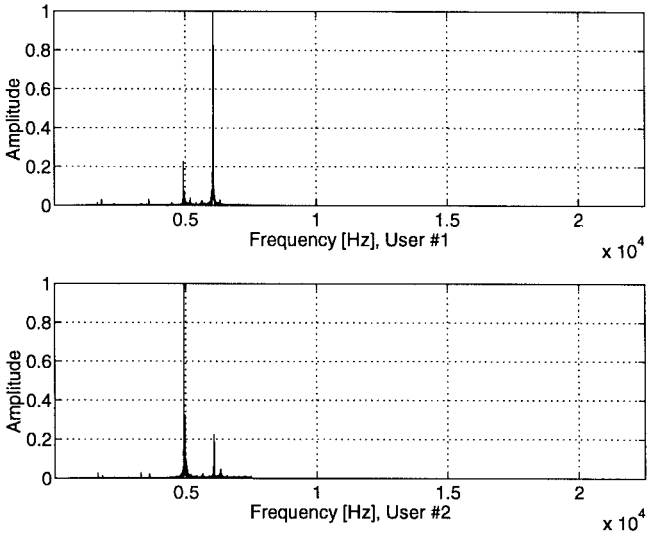

Fig. 20. SS-based beamforming results for two sources with angular separation of about 3°.

two mobile users and transmitted two user-specific tones back to the mobiles, applying their corresponding weighting vectors. Figs. 19 and 20 show the spectra of the signals received by the two mobile users with two different angular separations, 20° and 3°, respectively. We can see that the co-channel suppression achieved by spatial signatures downlink beamforming is quite significant (>13 dB) even when these two sources are very close.

V. Conclusion

The variation of the spatial signature with time, frequency, and small displacement was presented. Multipath angle spread and spatial signature-based beamforming performance were examined. We found that: 1) the variation of the spatial signature is very small if the mobile unit and its surroundings are stationary; 2) the spatial signature changes significantly with the carrier frequency; 3) the results of spatial signature variation with small displacement in different multipath environments show that there exists rich spatial diversity to be exploited by an antenna array for capacity expansion and performance improvement; 4) the angle spread of multipath is critical to the multipath fading characteristics of an antenna array as well as the feasibility of using direction finding techniques for selective uplinks and downlinks. The multipath angle spread is small in outdoors LOS environment while wider angle spread is observed in indoors and outdoors blocked environments; and 5) the co-channel suppression achieved by applying the spatial signature based on downlink beamforming is quite significant even if two mobile users are very close to each other.

From these experimental results we conclude that in a TDD system, spatial signature-based beamforming could achieve significant co-channel interference suppression even when the sources are very close to each other. In an FDD system, the spatial signature-based beamforming will not work since the downlink spatial signature will be significantly different from the uplink spatial signature due to the frequency difference of the links. In a TDD system, spatial signature-based beamforming is very suitable to communications applications, e.g. PCS, wireless PBX/LAN, and wireless static networks, where the mobile units do not move rapidly.

References

[1] S. C. Swales, M. A. Beach, D. J. Edwards, and J. P. McGreehan, "The performance enhancement of multibeam adaptive base-station antennas for cellular land mobile radio systems," *IEEE Trans. Veh. Technol.*, vol. 39, pp. 56–67, Feb. 1990.

[2] P. Balaban and J. Salz, "Optimum diversity combining and equalization in digital data transmission with applications to cellular mobile radio—Part I: Theoretical considerations," *IEEE Trans. Commun.*, vol. 40, pp. 885–894, May 1992.

[3] G. Xu, Y. Cho, A. Paulraj, and T. Kailath, "Maximum likelihood detection of co-channel communication signals via exploitation of spatial diversity," in *Proc. 26th Asilomar Conf. Signals, Syst., Comput.*, Pacific Grove, CA, Oct. 1992, pp. 1142–1146.

[4] J. H. Winters, J. Salz, and R. D. Gitlin, "The capacity of wireless communication systems can be substantially increased by the use of antenna diversity," in *Proc. 1st Int. Conf. Universal Personal Comun. ICUPC*, Dallas, TX, Sept. 29–Oct. 1, 1992, pp. 442–447.

[5] B. Suard, A. F. Naguib, G. Xu, and A. Paulraj, "Performance of CDMA mobile communication systems using antenna arrays," in *Proc. Int. Conf. Acoust., Speech, Signal Processing*, Minneapolis, MN, Apr. 1993, vol. 4, pp. 153–156.

[6] L. Tong, G. Xu, and T. Kailath, "Fast blind equalization of multipath channels via antenna arrays," in *Proc. Int. Conf. Acoust., Speech, Signal Processing*, Minneapolis, MN, Apr. 1993, pp. 272–275.

[7] G. Xu, H. Liu, W. J. Vogel, H. P. Lin, S. S. Jeng, and G. W. Torrence, "Experimental studies of space-division-multiple-access schemes for spectral efficient wireless communications," in *Proc. Int. Conf. Commun.*, New Orleans, LA, May 1994, vol. 2, pp. 800–804.

[8] S. S. Jeng, H. P. Lin, G. Xu, and W. J. Vogel, "Measurements of spatial signature of an antenna array," in *Proc. 6th Int. Symp. Personal, Indoor, Mobile Radio Commun.*, Toronto, ON, Canada, Sept. 1995, vol. 2, pp. 669–672.

[9] A. Paulraj, R. Roy, and T. Kailath, "A subspace rotation approach to signal parameter estimation," *Proc. IEEE*, vol. 74, pp. 1044–1045, July 1986.

[10] T. J. Shan, A. Paulraj, and T. Kailath, "On smoothed rank profile test in eigenstructure methods to direction-of-arrival estimation," *IEEE Trans. Acoust., Speech, Signal Processing*, vol. 33, pp. 1377–1385, Oct. 1987.

[11] S. U. Pillai and B. H. Kwon, "Forward/backward spatial smoothing techniques for coherent signal identification," *IEEE Trans. Acoust., Speech, Signal Processing*, vol. 37, no. 1, pp. 8–15, Jan. 1989.

Shiann-Shiun Jeng was born in Kaohuiung, Taiwan, on October 18, 1960. He received the B.S. and the M.S. degrees in telecommunication engineering from National Chiao-Tung University, Taiwan, in 1983 and 1985, respectively, and the Ph.D. degree in electrical engineering from The University of Texas, Austin, in 1997.

From 1985 to 1992 he was an Assistant Researcher in the Telecommunication Laboratories, Ministry of Transportations and Communications, Taiwan. In August 1997 he joined the faculty of the Department of Electronic Engineering, Chung Yuan University, Chungli, Taiwan, where he is currently an Assistant Professor. His research interests include channel propagation study, RF circuit design, wireless communications, and smart antenna systems.

Guanghan Xu (S'86–M'92) was born on November 10, 1962 in Shanghai, China. He received the B.S. degree with honors in biomedical engineering from Shanghai Jiao Tong University, Shanghai, China, in 1985, the M.S. degree in electrical engineering from Arizona State University, Tempe, AZ, in 1988, and the Ph.D. degree in electrical engineering from Stanford University, Stanford, CA, in 1991.

During the summer of 1989, he was a Research Fellow at Institute of Robotics, Swiss Institute of Technology, Zurich, Switzerland. From 1990 to 1991 he was a General Electric Fellow of Fellow-Mentor-Advisor Program at Center of Integrated Systems, Stanford University. From 1991 to 1992 he was a Research Associate in Department of Electrical Engineering, Stanford University and a short-term Visiting Scientist at the Laboratory of Information and Decision Systems of the Massachusetts Institute of Technology. In 1992 he became Assistant Professor of the Department of Electrical and Computer Engineering of The University of Texas at Austin. He was promoted to Associate Professor in 1997. He has worked in several areas including communications, signal processing, information theory, numerical linear algebra, multivariate statistics, and semiconductor manufacturing. His current research interest is focused on smart antenna systems for wireless communications.

Dr. Xu is a member of Phi Kappa Phi and is a recipient of the 1995 NSF CAREER Award and 1997 IEEE TRANSACTIONS ON SIGNAL PROCESSING Young Author Best Paper Award. He was a guest editor of a Special Issue of IEEE TRANSACTIONS ON SIGNAL PROCESSING and was elected a member of IEEE Committee on Array and Statistical Signal Processing.

Hsin-Piao Lin was born in Chia-yi, Taiwan. He received the B.S. degree in communication engineering from the National Chiao-Tung University, Taiwan, in 1986, and the M.S. and Ph.D. degrees from the University of Texas at Austin, in 1992 and 1997, respectively.

Since 1997, he has been an Assistant Professor in the Department of Electronic Engineering of the National Taipei University of Technology, Taipei, Taiwan. His current research interests are in the area of wireless communications, smart antenna systems, land-mobile satellite communications, and propagation channel modeling.

Wolfhard J. Vogel (S'69–M'74–SM'90–F'94) received the Vordiplom degree in electrical engineering from the Technical University of Berlin, Germany, and the M.S. and Ph.D. degrees in electrical engineering from the University of Texas, Austin, in 1969 and 1973, respectively.

He is currently an Associate Director of the Electrical Engineering Research Laboratory at the University of Texas, Austin. He has worked in the area of satellite-earth wave propagation research, emphasizing rain attenuation, depolarization effects, and fading due to shadowing and multipath for land-mobile and personal satellite communications from UHF to K-band. His current interests include characterizing propagation phenomena pertinent to satellite sound broadcasting, personal satellite communications systems, and smart antennas.

Dr. Vogel is Chairman for Commission F of the United States National Committee of the International Union of Radio Science (wave propagation and remote sensing) and chairs the IEEE Wave Propagation Standards Committee.